Epitaxial growth and properties of lead-free ferroelectric Na0.5Bi0.5TiO3 thin films grown by pulsed laser deposition on various single crystal substrates

F. Jean, M. Bousquet, Jean-René Duclere, Alexandre Boulle, R. Remondiere, S. Deputier, Jean-Christophe Orlianges, Pascal Marchet, Maryline Guilloux-Viry

Epitaxial growth and properties of lead-free ferroelectric $Na_{0.5}Bi_{0.5}TiO_3$ thin films grown by Pulsed Laser Deposition on various single crystal substrates

F. Jean[1], M. Bousquet[1,*], J.-R. Duclère[1], A. Boulle[1], F. Rémondière[1], S. Députier[2], J.-C. Orlianges[1], P. Marchet[1], M. Guilloux-Viry[2]

[1]Laboratoire de Sciences des Procédés Céramiques et de Traitements de Surface UMR 7315 CNRS Université de Limoges, Limoges, France

[2]Unité Sciences Chimiques de Rennes, UMR 6226 CNRS Equipe Chimie du Solide et Matériaux Université Rennes 1

[3]CC-MEM, Institut Jean Lamour, UMR 7198 CNRS – Nancy Université - UPV Metz Ecole des Mines Nancy, France

Current address: Laboratoire de Physique de la Matière Condensée, EA 2081, Université de Picardie Jules Verne, 33, rue Saint-Leu, 80039 Amiens Cedex, France

Abstract — **The epitaxial growth of lead-free ferroelectric $Na_{0.5}Bi_{0.5}TiO_3$ (NBT) thin films on various single crystal substrates was successfully achieved, using the pulsed laser deposition technique (PLD). The present work is divided in two parts, focused on: (i) the growth of NBT layers on *c*- and *r*-sapphire (Al_2O_3) substrates, with and without introducing a CeO_2 buffer layer, and (ii) the growth of NBT layers on bare (00l)$SrTiO_3$ substrates, with and without introducing a $LaNiO_3$ layer, that could be used as a bottom electrode. In the first part, it was shown that the introduction of a CeO_2 buffer layer completely modifies the out-of-plane growth orientation of the NBT films, as well as their microstructure. Indeed, (00l)NBT films epitaxially grow only on *r*-Al_2O_3 substrates buffered with epitaxial (00l)CeO_2 layers, while, growing simply NBT on top of bare *c* or *r*-Al_2O_3 substrates, or on top of CeO_2/*c*-Al_2O_3 heterostructures leads to polycrystalline or textured films. In the second part, we demonstrate that (00l)-oriented NBT layers deposited on either bare (00l)$SrTiO_3$ or (00l)$SrTiO_3$ substrates (STO) covered with (00l)$LaNiO_3$ (LNO) are systematically epitaxially grown. Furthermore, the microstructure of the samples is strongly affected by the introduction of the $LaNiO_3$ layer.**

Keywords- Keywords: $Na_{0.5}Bi_{0.5}TiO_3$, lead-free ferroelectrics, epitaxial thin films, optical properties

I. INTRODUCTION

Currently, lead-based compounds such as lead zirconate titanate $Pb(Zr,Ti)O_3$ (PZT) constitute the best family of piezoelectric and ferroelectric materials suitable for integration in devices, such as piezoelectric actuators, sensors and transducers [1]. However, due to health care and environmental problems, lead content must be reduced in such applications. Since the last ten years, many efforts have been devoted in the field of lead-free materials [2]. Among the different lead-free materials available for substitution of the PZT's family, $Na_{0.5}Bi_{0.5}TiO_3$ (NBT) appears as a promising candidate on account of its good ferroelectric (P_r = 38 μC/cm^2, E_c = 73 kV/cm) and piezoelectric properties (d_{33} = 79 pC/N) [3]. Since its discovery, many reports have been devoted to the study of structural and electrical properties of NBT in bulk form, but the literature dealing with thin films of pure NBT, NBT-based solid solutions, and heterostructures including NBT is obviously more restricted, most of the available references being published within the last ten years.

We are particularly interested in the elaboration of NBT thin films epitaxially grown on different substrates with different crystalline orientations, in order to access the physical properties, both at macroscopic and nanoscale level, and their relationships with crystalline structure and orientation [4-6]. The present work is particularly focused on: (i) the growth of NBT layers on *c*- and *r*-sapphire (Al_2O_3) substrates, with and without introducing a CeO_2 buffer layer and (ii) the growth of NBT layers on bare (00l)$SrTiO_3$ substrates, with and without introducing a $LaNiO_3$ layer

II. EXPERIMENTAL PROCEDURE

NBT thin films were grown by Pulsed Laser Deposition (PLD) from a home-made sintered target using a KrF laser (248nm) with a laser fluence of ~4 J/cm^2, and a repetition rate of 5 Hz, at a deposition temperature of 600°C under an oxygen pressure of 2.10^{-1} mbar. For the NBT/CeO_2 heterostructures fabrication, the different materials were deposited successively. X-ray diffraction (XRD) measurements were carried out using a θ / 2θ diffractometer operated with the Cu $K_{\alpha 1}$ radiation. φ-scans were also performed by using a 4-circle high resolution diffractometer in order to study the in-plane ordering of the films. Reciprocal space mapswere also finally recorded in order to extract both the in-plane and out-of-plane NBT lattice constants.. As the NBT unit cell is rhomboedral but with very small distortion (α = 89.8°), the (hkl) Miller indices

indexations are systematically reported using a pseudo-cubic system. Both field-emission scanning electron microscopy (FE-SEM) and Atomic Force Microscopy (AFM) were employed to observe the surface morphologies of the NBT films.

III. RESULTS

A. *NBT films grown on R and C-sapphire substrates*

XRD patterns reveal that NBT films grown on *c*-sapphire are polycrystalline, while a stronger (00l) texture is reached when growing on *r*-sapphire (fig.1). SEM pictures shows a change of the microstructure with the orientation of the substrate: when growing on *c*-sapphire, some cracks are observed while more homogeneous microstructure, with smaller grains, was evidenced for *c*-sapphire (fig.2).

B. *CeO_2 films grown on sapphire*

CeO_2 layers were deposited as well on *r*-and *c*-sapphire by PLD. After *in-situ* deposition at 700°C under an O_2 pressure of 0.4 mbar (1 min 30 sec at 2 Hz), the films were *ex-situ* annealed, at 800°C for two hours, under air atmosphere. SEM pictures (not shown here) revealed that the films are not continuous, due to the combined short deposition time and natural dewetting process. In addition, it is shown that the aspect of the microstructure depends on the substrate orientation. The XRD data indicate a mixture of mainly (111) and (00l) out-of-plane orientations. Moreover, CeO_2 films grown on top of *r*-sapphire substrates present a stronger (00l) texture (fig. 3). For this sample, the thickness of the CeO_2 layer was calculated to be ~ 13 nm, using the Laue-oscillations evidenced in the XRD patterns, in good agreement with the AFM data (12 nm, not shown here).

C. *NBT/CeO_2/sapphire heterostructures*

NBT/CeO_2/sapphire hetereostructures were elaborated by the consecutive deposition of CeO_2 layer, ex-situ annealed as describe above, followed by that of NBT layer. For the sample elaborated on *c*-sapphire, XRD patterns (fig. 3) show that the out-of-plane orientation of the CeO_2 layer is now purely (111), with a top NBT layer presenting some (011) texture. For the sample elaborated on *r*-sapphire, the unique out-of-plane orientation of both the CeO_2 and NBT layers appears to be (00l) (fig. 3).

As well, for the NBT/CeO_2/*c*-sapphire heterostructure, X-ray measurements performed in φ-scan mode reveal an epitaxial growth of the CeO_2 layer,with nevertheless some restricted quality, explaining why no in-plane ordering was evidenced for the NBT layer.

In the case of the NBT/CeO_2/*r*-sapphire heterostructure, epitaxial growth of both the CeO_2 and NBT layers was detected, with a fourfold symmetry (fig. 4). A 45° in-plane rotation of the NBT unit cell (a = 3.890 Å) with respect to that of CeO_2 (a = 5.412 Å) was evidenced, in agreement with the crystal lattices of the two materials. Optical measurements were carried out on these two samples by spectroscopic ellipsometry. After the extraction of the dispersion curves for both refractive (n) and extinction (k) indices, an optical band gap value in the order of 3.2 eV was extracted, in good agreement with the bulk NBT value. The calculated thicknesses of the samples are consistent with the other measurements (~ 100 nm for NBT and ~ 12 nm for CeO_2).

In the case of *c*-sapphire substrates, the observation of the microstructures by SEM reveals a drastic change of the microstructure of NBT films with the insertion of the CeO_2 buffer layer (fig. 5). In the case of *r*-sapphire substrates, the surface aspect of NBT films is not as much affected by the introduction of the CeO_2 buffer layer: however, films appear to be more homogeneous and show a much nicer aspect.

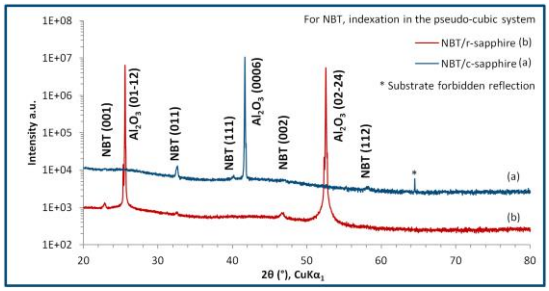

Fig.1: θ/2θ XRD patterns of NBT layers deposited on (a) *c*-sapphire and (b) *r*-sapphire single crystal substrates. The "*" symbol labels a forbidden reflection of the Al_2O_3 substrate.

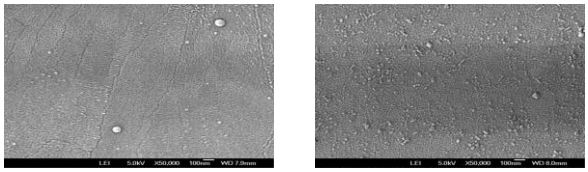

Fig.2: SEM images of NBT thin films grown on *c*– sapphire (left) and *r*-sapphire (right) substrates.

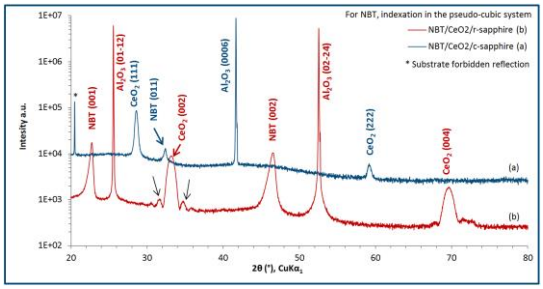

Fig.3: θ/2θ XRD patterns of CeO_2 layers grown on (a) *c*-sapphire and (b) *r*-sapphire single crystal substrates. The arrows highlight the Laüe oscillations.

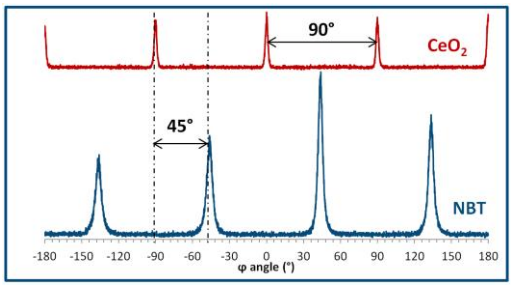

Fig.4: NBT/ CeO_2/sapphire heterostructures: XRD patterns collected in φ-scan mode and acquired on the (220)CeO_2 and the (110)NBT reflections.

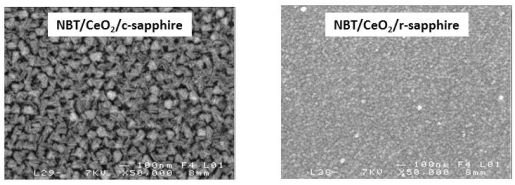

Fig.5: SEM images of the NBT/CeO_2/sapphire heterostructures.

D. NBT layers grown on (001)$SrTiO_3$

The XRD pattern of the NBT thin film deposited on (00l) $SrTiO_3$(STO) reveals a unique (00l) out-of-plane orientation (fig. 6.). The NBT pseudo-cubic lattice parameter calculated from the 2θ angle position of the (00l) Bragg peaks is 3.894 Å, *i.e.* extremely close to that of bulk NBT, meaning that the films are strain free and reflecting as well the perfect matching (- 0.4 %) of the two perovskite lattices. The Electron Channeling Pattern (ECP) presents a fourfold symmetry, thus proving the expected epitaxial growth of the NBT lattice on top of that of STO (fig.7).

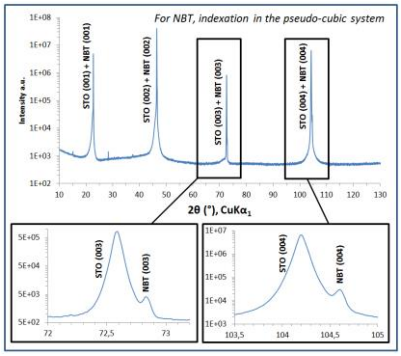

Fig.6: θ/2θ XRD pattern measured for the NBT film directly deposited on STO. The insets correspond to an enlargement around the (003) and (004) STO and NBT Bragg peaks, respectively.

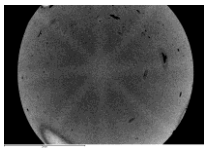

Fig.7: ECP acquired for the NBT/STO film

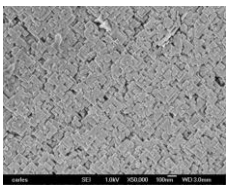

Fig.8: SEM image of the NBT/LNO/(001)STO heterostructure.

E. NBT/LNO/(001)STO heterostructures

The SEM image of the surface of NBT/LNO/(001)STO heterostructure reveals a change of the microstructure with the insertion of the LNO layer, compared to that observed for NBT films directly deposited on top of STO (fig. 8). The XRD pattern performed in θ/2θ mode shows also a unique (00l) outofplane orientation of the NBT layer (fig. 9), *i.e.* unchanged by the introduction LNO intermediate layer. XRD reciprocal space mapping demonstrates the epitaxy of both LNO and NBT layers (fig. 10). The calculation of the LNO and NBT lattice parameters reveals a deformation of both LNO and NBT lattices; the former being under tensile strains in order to accommodate the lattice parameter of STO. As a consequence, the in-plane NBT lattice parameters also match those of the LNO layer.

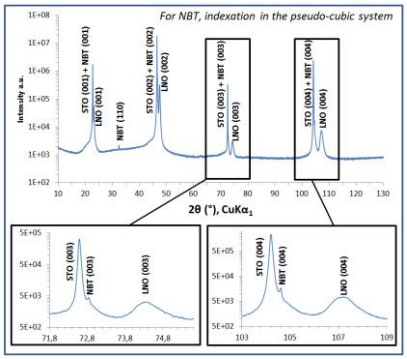

Fig.9: θ/2θ XRD pattern of the NBT/LNO/(001) STO heterostructure. The insets correspond to an enlargement around the (003) and (004) STO, NBT and LNO Bragg peaks, respectively.

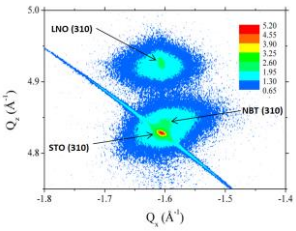

Fig.10: XRD reciprocal space mapping showing the (310) reciprocal lattice points of STO, NBT and LNO

IV. CONCLUSION

We have demonstrated the possibility for the epitaxial growth of NBT layers directly on STO substrates, as well as on epitaxial LNO layers supported by STO substrates and finally, that the insertion of an epitaxial CeO_2 layer deposited on *r*-sapphire allows the epitaxial growth of (00l)-oriented NBT crystallites. Furthermore, it was shown that the insertion of either CeO_2 or LNO buffer layers could induce a strong modification of the aspect of NBT films' microstructure. Future research would be to employ the LNO layer as a bottom electrode to conduct some electrical measurements of the samples.

[1] F. Levassort, P. Tran-Huu-Hue, E. Ringaard, and M. Lethiecq, J. Eur. Ceram. Soc. 21,

[2] J. Rödel, W. Jo, K. T. P. Seifert, E.-M. Anton, T. Granzow, and D. Damjanovic, J. Am.

[3] Y. Hiruma, H. Nagata and T. Takenaka, J. Appl. Phys. 105, 084112 (2009).

[4] J.-R. Duclère, C. Cibert, A. Boulle, V. Dorcet, P. Marchet, C. Champeaux, A. Catherinot, S. Deputier, M. Guilloux-Viry, Thin Solid Films 517, 592-597 (2008)

[5] M. Bousquet, J.-R. Duclère, C. Champeaux, A. Boulle, P. Marchet, A. Catherinot,A. Wu, P.M. Vilarinho, S. Deputier, M. Guilloux-Viry,A. Crunteanu, B. Gautier, D. Albertini, C. Bachelet, J. Appl. Phys. 107, 034102 (2010)

[6] M. Bousquet, J.-R. Duclère, E. Orhan, A. Boulle, C. Bachelet, C. Champeaux, J. Appl. Phys. 107, 104107 (2010)